

1 Experimental Determination of Solubilities of Tri-calcium Di-
2 Citrate Tetrahydrate $[Ca_3[C_3H_5O(COO)_3]_2 \cdot 4H_2O]$, Earlandite, in
3 NaCl and $MgCl_2$ Solutions to High Ionic Strengths and Its Pitzer
4 Model: Applications to Nuclear Waste Isolation and Other Low
5 Temperature Environments

6

7 Yongliang Xiong¹, Leslie Kirkes, Terry Westfall, Cassandra Marrs, Jandi Knox, Heather

8

Burton

9

Sandia National Laboratories (SNL)

10

Carlsbad Programs Group

11

4100 National Parks Highway, Carlsbad, NM 88220, USA

12

¹ Corresponding author, e-mail: yxiong@sandia.gov.

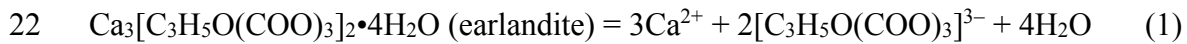
13

14 ABSTRACT

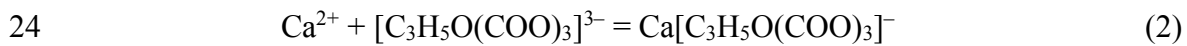
15 In this study, solubility measurements on tri-calcium di-citrate tetrahydrate
16 $[\text{Ca}_3[\text{C}_3\text{H}_5\text{O}(\text{COO})_3]_2 \cdot 4\text{H}_2\text{O}]$, abbreviated as $\text{Ca}_3[\text{Citrate}]_2 \cdot 4\text{H}_2\text{O}$ as a function of ionic
17 strength are conducted in NaCl solutions up to $I = 5.0 \text{ mol} \cdot \text{kg}^{-1}$ and in MgCl_2 solutions
18 up to $I = 7.5 \text{ mol} \cdot \text{kg}^{-1}$, at room temperature ($22.5 \pm 0.5^\circ\text{C}$). The solubility constant
19 ($\log K_{sp}^0$) for $\text{Ca}_3[\text{Citrate}]_2 \cdot 4\text{H}_2\text{O}$ and formation constant ($\log \beta_1^0$) for $\text{Ca}[\text{C}_3\text{H}_5\text{O}(\text{COO})_3]^-$

20 ,

21



23



25

26 are determined as -18.11 ± 0.05 and 4.97 ± 0.05 , respectively, based on the Pitzer model
27 with a set of Pitzer parameters describing the specific interactions in NaCl and MgCl_2
28 media.

29

The solubility measurements and thermodynamic modeling indicate that
30 $\text{Ca}_3[\text{Citrate}]_2 \cdot 4\text{H}_2\text{O}$ could become a solubility-controlling phase for citrate in geological
31 repositories for nuclear waste when the inventories of citrate reach the saturation
32 concentrations for $\text{Ca}_3[\text{Citrate}]_2 \cdot 4\text{H}_2\text{O}$.

33

34 1. INTRODUCTION

35 Citric acid (chemical formula, $C_6H_8O_7$, or structural formula, CH_2COOH-
36 $C(OH)COOH-CH_2COOH$, and its dissociated forms such as $[C_3H_5O(COO)_3]^{3-}$,
37 abbreviated as “Citrate” hereafter) is present in nuclear waste streams (Brush and
38 Xiong, 2009), as citrate is used in decontamination processes in the nuclear field
39 (Hummel et al., 2005). Therefore, it has a significant effect on the Performance
40 Assessment (PA) for the geological repositories for nuclear waste because of its ability to
41 form relatively strong aqueous complexes with actinides, especially actinides in the +III
42 oxidation state, potentially increasing solubilities of actinides. The strength of citrate
43 aqueous complexes with actinides is only second to those of EDTA with actinides. More
44 importantly, citrate has usually a higher inventory than EDTA, resulting in potentially
45 higher concentrations. As an example, the 2009 citrate inventory in the form of
46 $NaH_2Citrate$ and citric acid for the Waste Isolation Pilot Plant (WIPP), a U.S. DOE
47 geological repository for defense-related transuranic (TRU) waste, was 8.23×10^3 kg for
48 the 2009 Compliance Recertification Application Performance Assessment Baseline
49 Calculations (CRA-2009 PABC) (Brush and Xiong, 2009), and the calculated citrate
50 concentration in brines for CRA-2009 was $2.38 \times 10^{-3} \text{ mol}\cdot\text{dm}^{-3}$
51 (Brush and Xiong, 2009), higher than EDTA concentration (Brush and Xiong, 2009).

52 In addition, citrate is naturally present in other low temperature environments, and
53 therefore it plays an important role in mobilization of metals in low temperature
54 environments such as metallurgical slags (e.g., Ettler et al., 2004).

55 Earlandite was found in the Weddell Sea, Antarctic (Bannister and Hey, 1936;
56 Rex et al., 1970). The formation of earlandite in nature suggests that it is a stable phase

57 in natural environments, indicating that it has relatively low solubilities. This means that
58 earlandite could be a solubility-controlling phase for citrate in low temperature
59 environments. However, the solubility of earlandite as a function of ionic strength is not
60 well known in media that are important to geochemical processes. Such knowledge is
61 required for geochemical modeling of natural waters which may vary from dilute surface
62 and groundwater to highly concentrated brines saturated. Therefore, the objective of this
63 work is to determine solubilities of earlandite as a function of ionic strength to 5.0
64 mol•kg⁻¹ in a NaCl medium, and to 7.5 mol•kg⁻¹ in MgCl₂ medium, as NaCl and MgCl₂
65 are the most common and important components in natural aqueous systems, and they are
66 dominant components in the WIPP Generic Weep Brine (GWB) and Energy Research
67 and Development Administration Well 6 (ERDA-6) (Xiong and Lord, 2008). Based on
68 the measured solubilities, a Pitzer model was developed here for solubilities of earlandite,
69 and the interactions of citrate with NaCl and MgCl₂ media. The model would enable
70 researchers to estimate with a degree of high precision regarding solubilities of earlandite
71 in various environments over a wide range of ionic strengths.

72

73

74 2. EXPERIMENTAL SECTION

75

76 In these solubility experiments, about 2 grams of the starting material—ACS
77 reagent grade tri-calcium di-citrate tetrahydrate (Ca₃[Citrate]₂•4H₂O, earlandite, CAS
78 5785-44-4) from ACROS ORGANICS was weighed out and placed into 150 mL plastic
79 bottles. Then, 100 mL of supporting electrolyte solution were added to those bottles.
80 Once filled, the lids of the bottles were sealed with parafilm.

81 The supporting electrolytes are a series of NaCl solutions ranging from 0.010
82 mol•kg⁻¹ to 5.0 mol•kg⁻¹, and MgCl₂ solutions ranging from 0.01 mol•kg⁻¹ to 2.5
83 mol•kg⁻¹. The supporting electrolyte solutions were prepared from degassed deionized
84 (DI) water. The degassed DI water was prepared by following a procedure similar to that
85 used by Wood et al. (2002) to remove dissolved CO₂. The undersaturation experiments
86 are conducted at laboratory room temperature (22.5 ± 0.5°C).

87 The pH readings were measured with an Orion-Ross combination pH glass
88 electrode, coupled with an Orion Research EA 940 pH meter that was calibrated with
89 three pH buffers (pH 4, pH 7, and pH 10). In solutions with an ionic strength higher than
90 0.10 mol•kg⁻¹, hydrogen-ion concentrations on molar scale (pCH) were determined from
91 pH readings by using correction factors for NaCl and MgCl₂ solutions determined by Rai
92 et al. (1995) and Hansen (2001), respectively. Based on the equation in Xiong et al.
93 (2010), pCHs are converted to hydrogen-ion concentrations on the molal scale (pmH) (see
94 details in footnotes for Tables 1 and 2).

95 Solution samples were periodically withdrawn from experimental runs. Before
96 solution samples were taken, pH readings of experimental runs were measured. The
97 sample size was usually 3 mL. After a solution sample was withdrawn from an
98 experiment and filtered with a 0.2 µm syringe filter, the filtered solution was then
99 weighed, acidified with 0.5 mL of concentrated TraceMetal[®] grade HNO₃ from Fisher
100 Scientific, and finally diluted to a volume of 10 mL with DI water. If subsequent
101 dilutions were needed, aliquots were taken from the first dilution samples for the second
102 dilution, and aliquots of the second dilution were then taken for further dilution.

103 Calcium concentrations of solutions were analyzed with a Perkin Elmer dual-view
104 inductively coupled plasma-atomic emission spectrometer (ICP-AES)
105 (Perkin Elmer DV 3300). Calibration blanks and standards were precisely matched with
106 experimental matrices. The linear correlation coefficients of calibration curves in all
107 measurements were better than 0.9995. The analytical precision for ICP-AES is better
108 than 1.00% in terms of the relative standard deviation (RSD) based on replicate analyses.
109 Stoichiometric dissolution of earlandite was confirmed by analyzing for citrate
110 concentrations with a DIONEX ion chromatograph (IC) (DIONEX IC 3000) for selected
111 samples.

112 Uncertainties are estimated using a method described in one of our previous
113 publications (i.e., Nemer et al., 2010).

114

115 3. EXPERIMENTAL RESULTS, AND THERMODYNAMIC MODELING

116 3.1 Experimental Results

117 Experimental results for solubilities in NaCl and MgCl₂ solutions are tabulated in
118 Tables 1 and 2, respectively. In Figure 1, solubilities of earlandite as a function of
119 experimental time in NaCl solutions are displayed. From Figure 1, it is clear that steady-
120 state concentrations in NaCl solutions are achieved in the second sampling, which was
121 taken at 375 days (Table 1). Solubilities of earlandite as a function of experimental time
122 in MgCl₂ solutions are displayed in Figure 2. It is clear from Figure 2 that steady-state
123 concentrations in MgCl₂ solutions are achieved in the first sampling, which was taken at
124 385 days (Table 2). It is assumed that steady-state concentrations represent equilibrium
125 concentrations, as the duration of experiments in this work, up to 1,067 days, is
126 significantly longer than previous studies under similar conditions. For instance, in the
127 experiments of Vavrusova and Skibsted (2016), they mentioned that equilibrium was
128 established in several hours in their study.

129 In Figure 3, concentrations of calcium as a function of molalities of NaCl are
130 displayed. Figure 3 indicates that concentrations of calcium in equilibrium with
131 earlandite have a dependence on concentrations of NaCl. The calcium concentrations
132 first increase with NaCl molality.

133 Similarly, concentrations of calcium as a function of ionic strength in MgCl₂
134 solutions are displayed in Figure 4. Figure 4 suggests that concentrations of calcium in
135 equilibrium with earlandite have a dependence on concentrations of MgCl₂ with rising
136 solubilities with increasing MgCl₂ concentrations up to 1.0 mol•kg⁻¹. Above 1.0

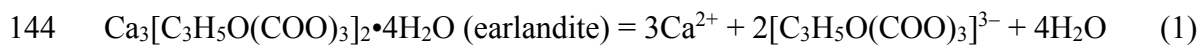
137 mol•kg⁻¹ regarding molality of MgCl₂, the dependence of solubility on ionic strength
138 become weaker, indicating a weaker, negative dependence on ionic strength.

139

140 3.2 Thermodynamic Modeling

141 In the following, the experimental data described above are used to derive the
142 thermodynamic parameters. The dissolution of earlandite can be expressed as,

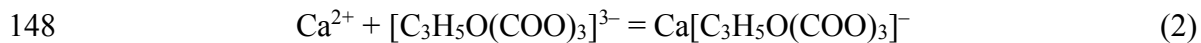
143



145

146 At the same time, the formation of CaCitrate⁻ complex can be expressed as,

147



149

150 Using experimental data produced in this study, the solubility constant of
151 earlandite related to Reaction (1) and formation constant related to Reaction (2) along
152 with a set of Pitzer parameters are obtained (Table 3), based on thermodynamic modeling
153 with the Pitzer equations. The auxiliary parameters are listed in Table 3. The computer
154 code, EQ3/6 Version 8.0a (Wolery et al., 2010; Xiong, 2011), is used as the modeling
155 platform, which was also used in previous modeling work for obtaining thermodynamic
156 properties including the Pitzer parameters (e.g., Xiong et al., 2013, 2017; Xiong, 2013,
157 2015). The database containing all parameters necessary including thermodynamic
158 properties for the modeling, is the fm1 database (data0.fm1) (Xiong, 2011). In the fm1

159 database, the interaction parameters for major ions are from Harvie et al. (1984), and the
160 interaction parameters for organic ligands are from Choppin et al. (2001).

161 In the model fitting, the experimental data were first used to generate EQ3/6 input
162 files. Then, a script such as a Python script was generated to call the targeted parameters,
163 and call EQ3/6. The minimization subroutine in the script automatically compares total
164 sum of squared residuals between experimental values [i.e., total calcium concentrations,
165 $\Sigma\text{Ca(II)}/\text{mol}\cdot\text{kg}^{-1}$] and model-predicted values produced by each set of adjusted
166 parameters in each iteration. The iteration is completed when the total sum of squared
167 residuals reaches a minimum.

168 In Table 3, the dissolution constant for earlandite, the formation constant for
169 CaCitrate^- , and a set of Pitzer parameters describing the specific interactions of citrate
170 species in NaCl and MgCl_2 media are listed. These Pitzer parameters are similar to those
171 found in the literature for the similar interactions in terms of magnitude. For instance, the
172 $\beta^{(0)}$ for Mg^{2+} — CaCitrate^- interaction, a 2:1 interaction, is 0.3760 (Table 3), which is
173 similar to the $\beta^{(0)}$ of 0.35235 for Mg^{2+} — Cl^- interaction (Harvie et al., 1984), also a 2:1
174 interaction. It is also similar to the $\beta^{(0)}$ of 0.32 for Na^+ — $\text{H}_2\text{SiO}_4^{2-}$ interaction (Hershey
175 and Millero, 1986), also a 1:2 interaction.

176 It is worth noting that the formation constant for CaCitrate^- obtained in this study
177 is in excellent agreement with the literature values. In this work, the derived $\log \beta_1^0$ is
178 4.97. The $\log \beta_1^0$ experimentally evaluated by Davies and Hoyle (1953) 4.90. This
179 agreement between the value determined in this study and those in the literature provide
180 the additional support for the model presented here.

181 In the NEA review, $\log \beta_1^0$ for CaCitrate^- has a value of 4.80 ± 0.03
182 (Hummel et al., 2005), evaluated with the SIT model. It is worth noting that the value
183 evaluated in the NEA review is based on experimental data in low ionic strength range,
184 i.e., predominantly at $0.1 \text{ mol}\cdot\text{kg}^{-1}$. The NEA review series also mentioned that when the
185 Pitzer and SIT models apply to the same data set for a reaction involving highly charged
186 species such as $\text{NpO}_2(\text{CO}_3)_3^{5-}$, to calculate activity coefficients, the $\log K^o$ can differ by
187 ~ 0.5 logarithmic units (Guillaumont et al., 2003). Therefore, it is expected that the
188 $\log \beta_1^0$ evaluated in this work using the Pitzer model based on a data set over a wide
189 range of ionic strengths would slightly differ from the value in the NEA review with the
190 SIT model based on a data set in low ionic strength range predominantly at $0.1 \text{ mol}\cdot\text{kg}^{-3}$.

191 The $\log K_{sp}^0$ presented in the NEA review was -17.9 ± 0.1 (Hummel et al., 2005),
192 using the SIT model for evaluation, based on the data limited to $I_m \leq 0.5 \text{ mol}\cdot\text{kg}^{-1}$ from
193 Ciavatta et al. (2001). The $\log K_{sp}^0$ obtained in this study is -18.11 ± 0.05 , agreeing with
194 the NEA value within the quoted uncertainties.

195 It should be noted that the $\beta^{(1)}$'s in Table 3 were not calculated. Instead, they are
196 pre-set to the average values for the respective interactions, following the paradigm of
197 Choppin et al. (2001). In Choppin et al. (2001), they calculated and recommended a set
198 of average values of $\beta^{(1)}$'s for various interactions (e.g., 1:1, 1:2/2:1, 1:3/3:1, etc.,
199 interactions), based on the $\beta^{(1)}$ values for respective interactions from literature.

200 In the following, solubilities of earlandite in a wide range of ionic strengths
201 predicted by the model are compared with experimental data. The solubilities of
202 earlandite as a function of ionic strength in a NaCl medium predicted by the model

203 developed in this study are represented by the solid curve in Figure 3. From Figure 3, it
204 is clear that the model developed in this study can accurately describe solubilities of
205 earlandite over a wide range of ionic strengths. There are few experimental studies on
206 solubility of earlandite.

207 Notice that the model-predicted values are in excellent agreement with the model-
208 independent solubility data of earlandite in water from Apelblat (1993), Vavrusova and
209 Skibsted (2016).

210 It is worth noting that the solubility behavior of earlandite in NaCl solutions is
211 different from that of $\text{Ca}_2\text{EDTA}\cdot 7\text{H}_2\text{O}(\text{s})$ in NaCl solutions (Xiong et al., 2017).
212 Regarding the solubility behavior of $\text{Ca}_2\text{EDTA}\cdot 7\text{H}_2\text{O}(\text{s})$ in NaCl solutions, the calcium
213 concentrations first increase with NaCl molality in the range of $0.01 \text{ mol}\cdot\text{kg}^{-1}$ to 1.0
214 $\text{mol}\cdot\text{kg}^{-1}$ (Xiong et al., 2017). Above $1.0 \text{ mol}\cdot\text{kg}^{-1}$, the calcium concentrations decrease
215 with increasing concentrations of NaCl (Xiong et al., 2017). In contrast, the calcium
216 concentrations in equilibrium with earlandite in NaCl solutions monotonically increase
217 with molality of NaCl. This is due to the strong interactions between Na^+ and Citrate^{3-}
218 (Gácsi et al., 2016), as indicated by the negative values of $\beta^{(0)}$ and C^ϕ for Na^+ —
219 $\text{Ca}[\text{C}_3\text{H}_5\text{O}(\text{COO})_3]^-$ (Table 3).

220 Similarly, the solubilities of earlandite as a function of ionic strength in an MgCl_2
221 medium predicted by the model developed in this study are represented by the solid curve
222 in Figure 4. It is clear from Figure 4 that the model developed in this study can
223 satisfactorily reproduce solubilities of earlandite in MgCl_2 solutions over a wide range of
224 ionic strengths. In the very high ionic strength range, the model predicts a slightly
225 stronger negative dependence on ionic strength in comparison with the experimental

226 results. In addition, in contrast with the trend in a NaCl medium, the solubility of
227 earlandite in a MgCl₂ medium does not change significantly with ionic strength at $I_m \geq 3$
228 mol•kg⁻¹.

229 The above thermodynamic modeling indicates that earlandite may be a solubility-
230 limiting phase for citric aqueous concentrations dominated by Na-Mg-Cl in geological
231 repositories when inventories of citrate increase to a level reaching the solubility limit of
232 citrate.

233

234 4. CONCLUSIONS

235 Long-term solubility measurements up to 1,067 days and to high ionic strengths
236 for earlandite in NaCl and MgCl₂ solutions produced at Sandia National Laboratories
237 Carlsbad Facility are presented in this work. A Pitzer model is developed based on these
238 solubility measurements. This model would provide accurate descriptions about the
239 interaction of citrate with NaCl, and satisfactory descriptions about the interaction of
240 citrate with MgCl₂, under various conditions with applications to many fields such as
241 nuclear waste management and environmental remediation of heavy metal contamination.

242

243 5. ACKNOWLEDGEMENTS

244 Sandia National Laboratories is a multimission laboratory managed and operated
245 by National Technology and Engineering Solutions of Sandia, LLC., a wholly owned
246 subsidiary of Honeywell International, Inc., for the U.S. Department of Energy's National
247 Nuclear Security Administration under contract DE-NA-0003525. This research is
248 funded by WIPP programs administered by the Office of Environmental Management

249 (EM) of the U.S Department of Energy. The laboratory assistance from Diana Goulding,
250 Brittany Hoard, Rachael Roselle, Tana Saul, and Kira Vicent is gratefully acknowledged.
251 The author is grateful to the journal reviewers for their insightful reviews which have
252 significantly improved the presentation. The author would like to thank Dr. Jeremy Fein,
253 the journal editor, for his editorial efforts and time.
254

255 REFERENCES

256

- 257 AI Mahamid, I., Novak, C.F., Becraft, K.A., Carpenter, S.A. and Hakem, N., 1998.
258 Solubility of Np (V) in K-Cl-CO₃ and Na-K-Cl-CO₃ Solutions to High
259 Concentrations: Measurements and Thermodynamic Model Predictions.
260 *Radiochimica Acta*, 81(2), pp.93-102.
- 261 Bannister, F.A. and Hey, M.H., 1936. Report on some crystalline components of the
262 Weddell Sea deposits. *Discovery Reports*, 13, pp.60-69.
- 263 Brush, L.H., and Xiong, Y.-L., 2009. Calculation of Organic-Ligand Concentrations for
264 the WIPP CRA-2009 PABC. Analysis Report, June 16, 2009. Carlsbad, NM: Sandia
265 National Laboratories. ERMS 551481.
- 266 Brush, L.H., Xiong, Y.-L., Long, J.J., 2009. Results of the Calculations of Actinide
267 Solubilities for the WIPP CRA-2009 PABC. Analysis Report, October 7, 2009.
268 Carlsbad, NM: Sandia National Laboratories. ERMS 552201.
- 269 Ciavatta, L., Tommaso, D., Iuliano, M., 2001. The solubility of calcium citrate hydrate in
270 sodium perchlorate solutions. *Analytical Letters*, 34:1053-1062.
- 271 Choppin G. R., Bond A. H., Borkowski M., Bronikowski M. G., Chen J.-F., Lis S.,
272 Mizera J. Pokrovsky O. S., Wall N. A., Xia Y.-X. and Moore, R. C. (2001) Waste
273 Isolation Pilot Plant Actinide Source Term Test Program: Solubility Studies and
274 Development of Modeling Parameters. Sandia National Laboratories Report.
275 SAND99-0943.
- 276 Davies, C.W. and Hoyle, B.E., 1953. 842. The interaction of calcium ions with some
277 phosphate and citrate buffers. *Journal of the Chemical Society (Resumed)*, pp.4134-
278 4136.
- 279 Ettler, V., Komárková, M., Jehlička, J., Coufal, P., Hradil, D., Machovič, V. and
280 Delorme, F., 2004. Leaching of lead metallurgical slag in citric solutions—
281 implications for disposal and weathering in soil environments. *Chemosphere*, 57(7),
282 pp.567-577.
- 283 Gácsi, A., Kutus, B., Buckó, Á., Csendes, Z., Peintler, G., Pálincó, I. and Sipos, P., 2016.
284 Some aspects of the aqueous solution chemistry of the Na⁺/Ca²⁺/OH⁻/Cit³⁻
285 system: The structure of a new calcium citrate complex forming under hyperalkaline
286 conditions. *Journal of Molecular Structure*, 1118, pp.110-116.

287

288

- 289 Guillaumont, R., Fanghänel, T., Neck, V., Fuger, J., Palmer, D.A., Grenther, I., Rand
290 M.H., 2003. Chemical Thermodynamics Vol. 5. Update on the Chemical
291 Thermodynamics of Uranium, Neptunium, Plutonium, Americium and Technetium.
292 Elsevier, Amsterdam.
- 293 Hansen, D.J., 2001. Determining aluminum solubilities as part of cement degradation
294 studies in support of the Waste Isolation Pilot Plant. SAND2001-2144P,
295 Albuquerque, NM: Sandia National Laboratories.
- 296 Harvie, C.E., Moller, N., Weare, J.H., 1984. The prediction of mineral solubilities in
297 natural waters: The Na-K-Mg-Ca-H-Cl-SO₄-OH-HCO₃-CO₃-CO₂-H₂O system to
298 high ionic strengths at 25°C. *Geochimica et Cosmochimica Acta* 48, 723–751.
- 299 Hershey, J.P., and Millero, F.J., 1986. The dependence of the acidity constants of silicic
300 acid on NaCl concentration using Pitzer's equation. *Marine Chemistry*, 18, 101–105.
- 301 Hummel, W., Anderegg, G., Puigdomenech, I., Rao, L., Tochiyama, O., 2005. Chemical
302 Thermodynamics of Compounds and Complexes of U, Np, Pu, Am, Tc, Zr, Ni and
303 Se with Selected Organic Ligands. Chemical Thermodynamics, Volume 9, OECD
304 Nuclear Energy Agency, Data Bank, Issy-les-Moulineaux, France, Elsevier B.V.
305 Amsterdam, The Netherlands, p. 1088.
- 306 Nemer, M.B., Xiong, Y., Ismail, A.E. and Jang, J.H., 2011. Solubility of Fe₂(OH)₃Cl
307 (pure-iron end-member of hibbingite) in NaCl and Na₂SO₄ brines. *Chemical
308 Geology*, 280(1), pp.26-32.
- 309 Rai, D., Felmy, A.R. Juracich, S.I., Rao, F.F., 1995. Estimating the hydrogen ion
310 concentration in concentrated NaCl and Na₂SO₄ electrolytes. SAND94-1949.
311 Sandia National Laboratories, Albuquerque, NM.
- 312 Rex, R.W., Margolis, S.V. and Murray, B., 1970. Possible interglacial dune sands from
313 300 meters water depth in the Weddell Sea, Antarctica. *Geological Society of
314 America Bulletin*, 81(11), pp.3465-3472.
- 315 Söhnel, O, Novotný, P., 1985. Densities of aqueous solutions of inorganic substances.
316 Elsevier, New York, 335 p.
- 317 Thakur, P., Xiong, Y.-L., Borkowski, M., and Choppin, G.R., 2014. Improved
318 thermodynamic model for interaction of EDTA with trivalent actinides and
319 lanthanide to ionic strength of 6.60 m. *Geochimica et Cosmochimica Acta* 133,
320 299–312.
- 321 U.S. DOE, 1996. Compliance Certification Application 40 CFR Part 191 Subpart B and
322 C U.S. Department of Energy Waste Isolation Pilot Plant. Appendix SOTERM.
323 DOE/CAO 1996-2184. Carlsbad, NM: U.S. DOE Carlsbad Area Office.

- 324 Vavrusova, M. and Skibsted, L.H., 2016. Aqueous solubility of calcium citrate and
325 interconversion between the tetrahydrate and the hexahydrate as a balance between
326 endothermic dissolution and exothermic complex formation. *International Dairy*
327 *Journal*, 57, pp.20-28.
- 328 Wolery, T.J., 1992. *EQ3/6, A Software Package for Geochemical Modeling of Aqueous*
329 *Systems: Package Overview and Installation Guide (Version 7.0)*, UCRL-MA-
330 *110662-PT-I* (Lawrence Livermore National Laboratory: Livermore, CA).
- 331 Wolery, T.J., Xiong, Y.-L., and Long, J. (2010) Verification and Validation
332 Plan/Validation Document for EQ3/6 Version 8.0a for Actinide Chemistry,
333 Document Version 8.10. Carlsbad, NM: Sandia National laboratories. ERMS
334 550239.
- 335 Wood, S.A., 2000. Organic matter: Supergene Enrichment and Dispersion, in *Ore*
336 *Genesis and Exploration: The Roles of organic matter. Reviews in Economic*
337 *Geology, Vol. 9* (Eds T. H. Giordano, R. M. Kettler, S. A. Wood), pp. 157–192
338 (Society of Economic Geologist, Littleton, CO).
- 339 Wood, S.A., Palmer, D.A., Wesolowski, D.J., Bénézech, P., 2002. The aqueous
340 geochemistry of the rare earth elements and yttrium. Part XI. The solubility of
341 $\text{Nd}(\text{OH})_3$ and hydrolysis of Nd^{3+} from 30 to 290°C at saturated water vapor pressure
342 with in-situ pHm measurement. In: Hellmann, R., Wood, S.A. (eds) *Water rock-*
343 *interactions, ore deposits, and environmental geochemistry: a tribute to David*
344 *Crerar, Special Publication 7. The Geochemical Society, St. Louis, Missouri, USA,*
345 *pp 229–256.*
- 346 Xiong, Y.-L., 2009. The aqueous geochemistry of thallium: speciation and solubility of
347 thallium in low temperature system. *Environmental Chemistry*, 6(5): 441–451.
- 348 Xiong, Y.-L., 2011. WIPP Verification and Validation Plan/Validation Document for
349 EQ3/6 Version 8.0a for Actinide Chemistry, Revision 1, Document Version 8.20.
350 Supersedes ERMS 550239. Carlsbad, NM. Sandia National Laboratories. ERMS
351 555358.
- 352 Xiong, Y.-L., 2013. An Aqueous Thermodynamic Model for Solubility of Potassium
353 Ferrate in Alkaline Solutions to High Ionic Strengths at 283.15 K to 333.15 K.
354 *Journal of Solution Chemistry* 42, 1393–1403.
- 355 Xiong, Y.-L., 2015. Experimental determination of lead carbonate solubility at high
356 ionic strengths: a Pitzer model description. *Monatshefte fuer Chemie/Chemical*
357 *Monthly*, 146:1433-1443.
- 358 Xiong, Y.-L., and Lord, A.C.S., 2008. Experimental investigations of the reaction path in
359 the $\text{MgO-CO}_2\text{-H}_2\text{O}$ system in solutions with ionic strengths, and their applications
360 to nuclear waste isolation. *Applied Geochemistry* 23, 1634–1659.

- 361 XIONG, Y., 2010, November. EXPERIMENTAL DETERMINATION OF
362 SOLUBILITY CONSTANT OF EARLANDITE ($\text{Ca}_3[\text{C}_3\text{H}_5\text{O}(\text{COO})_3]_2 \cdot 4\text{H}$
363 2O) AND PITZER INTERACTION PARAMETERS OF $\text{CaC}_3\text{H}_5\text{O}(\text{COO})_3$ -IN
364 $\text{NaCl-H}_2\text{O}$ AND $\text{MgCl}_2\text{-H}_2\text{O}$ SYSTEMS. In *2010 GSA Denver Annual*
365 *Meeting*.
- 366 Xiong, Y.-L., Deng, H.-R., Nemer, M., and Johnsen, S. (2010) Experimental
367 determination of the solubility constant for magnesium chloride hydroxide hydrate
368 ($\text{Mg}_3\text{Cl}(\text{OH})_5 \cdot 4\text{H}_2\text{O}$), phase 5) at room temperature, and its importance to nuclear
369 waste isolation in geological repositories in salt formations. *Geochimica et*
370 *Cosmochimica Acta*, 74, 4605-46011.
- 371 Xiong, Y.-L., Kirkes, L., and Westfall, T., 2013. Experimental Determination of
372 Solubilities of Sodium Tetraborate (Borax) in NaCl Solutions, and A
373 Thermodynamic Model for the $\text{Na-B}(\text{OH})_3\text{-Cl-SO}_4$ System to High Ionic Strengths
374 at 25 °C. *American Mineralogist* 98, 2030–2036.
- 375 Xiong, Y., Leigh, C.D. and Domski, P.S., 2016. *WIPP Thermodynamic Database History*
376 *and Recent Revisions* (No. SAND2016-1298PE). Sandia National Laboratories
377 (SNL-NM), Albuquerque, NM (United States); Sandia National Laboratories,
378 Albuquerque, NM.
- 379 Xiong, Y., Kirkes, L. and Westfall, T., 2017. Experimental determination of solubilities
380 of di-calcium ethylenediaminetetraacetic acid hydrate [$\text{Ca}_2\text{C}_{10}\text{H}_{12}\text{N}_2\text{O}_8 \cdot 7\text{H}$
381 2O (s)] in NaCl and MgCl_2 solutions to high ionic strengths and its Pitzer model:
382 Applications to geological disposal of nuclear waste and other low temperature
383 environments. *Chemical Geology*, 454, pp.15-24.
- 384

385
386
387
388

Table 1. Experimental results concerning solubility of earlandite, $\text{Ca}_3[\text{Citrate}]_2 \cdot 4\text{H}_2\text{O}(\text{s})$, in NaCl solutions produced at SNL at 22.5 ± 0.5 °C.

Experimental Number	Supporting Medium, NaCl, molal	Experimental time, days	pmH*	Solubility expressed as total calcium on molal scale, $m_{\Sigma\text{Ca}}$
ACROS-ELDT-0.01-1	0.010	182	6.98	5.23E-03
ACROS-ELDT-0.01-2	0.010	182	6.96	5.39E-03
ACROS-ELDT-0.1-1	0.10	182	6.48	7.25E-03
ACROS-ELDT-0.1-2	0.10	182	6.54	7.89E-03
ACROS-ELDT-1.0-1	1.0	182	6.42	1.38E-02
ACROS-ELDT-1.0-2	1.0	182	6.51	1.86E-02
ACROS-ELDT-2.0-1	2.1	182	6.09	1.56E-02
ACROS-ELDT-2.0-2	2.1	182	6.12	1.56E-02
ACROS-ELDT-3.0-1	3.2	182	5.51	2.87E-02
ACROS-ELDT-3.0-2	3.2	182	5.29	3.00E-02
ACROS-ELDT-5.0-1	5.0	182	4.92	NA
ACROS-ELDT-5.0-2	5.0	182	4.89	NA
ACROS-ELDT-0.01-1	0.010	375	7.15	4.65E-03
ACROS-ELDT-0.01-2	0.010	375	7.27	5.02E-03
ACROS-ELDT-0.1-1	0.10	375	6.86	6.93E-03
ACROS-ELDT-0.1-2	0.10	375	6.99	6.67E-03
ACROS-ELDT-1.0-1	1.0	375	6.77	1.20E-02
ACROS-ELDT-1.0-2	1.0	375	6.39	1.24E-02
ACROS-ELDT-2.0-1	2.1	375	5.83	1.44E-02
ACROS-ELDT-2.0-2	2.1	375	6.30	1.39E-02
ACROS-ELDT-3.0-1	3.2	375	5.61	2.35E-02
ACROS-ELDT-3.0-2	3.2	375	5.39	2.58E-02
ACROS-ELDT-5.0-1	5.0	375	4.69	3.15E-02
ACROS-ELDT-5.0-2	5.0	375	4.73	3.35E-02
ACROS-ELDT-0.01-1	0.010	662	7.55	4.84E-03
ACROS-ELDT-0.01-2	0.010	662	7.54	4.73E-03
ACROS-ELDT-0.1-1	0.10	662	7.38	6.75E-03
ACROS-ELDT-0.1-2	0.10	662	7.46	6.75E-03
ACROS-ELDT-1.0-1	1.0	662	7.16	1.18E-02
ACROS-ELDT-1.0-2	1.0	662	6.59	1.17E-02
ACROS-ELDT-2.0-1	2.1	662	5.99	1.78E-02
ACROS-ELDT-2.0-2	2.1	662	6.06	1.73E-02

ACROS-ELDT-3.0-1	3.2	662	5.99	2.63E-02
ACROS-ELDT-3.0-2	3.2	662	5.59	2.65E-02
ACROS-ELDT-5.0-1	5.0	662	4.81	3.45E-02
ACROS-ELDT-5.0-2	5.0	662	4.81	3.47E-02
ACROS-ELDT-0.01-1	0.010	712	7.69	5.07E-03
ACROS-ELDT-0.01-2	0.010	712	7.70	4.97E-03
ACROS-ELDT-0.1-1	0.10	712	7.54	6.80E-03
ACROS-ELDT-0.1-2	0.10	712	7.61	6.90E-03
ACROS-ELDT-1.0-1	1.0	712	7.29	1.16E-02
ACROS-ELDT-1.0-2	1.0	712	6.62	1.19E-02
ACROS-ELDT-2.0-1	2.1	712	6.05	1.77E-02
ACROS-ELDT-2.0-2	2.1	712	6.13	1.74E-02
ACROS-ELDT-3.0-1	3.2	712	6.08	2.64E-02
ACROS-ELDT-3.0-2	3.2	712	5.62	2.67E-02
ACROS-ELDT-5.0-1	5.0	712	4.69	3.42E-02
ACROS-ELDT-5.0-2	5.0	712	4.67	3.41E-02
ACROS-ELDT-0.01-1	0.010	760	7.68	5.20E-03
ACROS-ELDT-0.01-2	0.010	760	7.65	5.04E-03
ACROS-ELDT-0.1-1	0.10	760	7.67	6.99E-03
ACROS-ELDT-0.1-2	0.10	760	7.64	6.79E-03
ACROS-ELDT-1.0-1	1.0	760	7.28	1.17E-02
ACROS-ELDT-1.0-2	1.0	760	6.57	1.20E-02
ACROS-ELDT-2.0-1	2.1	760	6.10	1.79E-02
ACROS-ELDT-2.0-2	2.1	760	6.17	1.73E-02
ACROS-ELDT-3.0-1	3.2	760	6.20	2.60E-02
ACROS-ELDT-3.0-2	3.2	760	6.13	2.61E-02
ACROS-ELDT-5.0-1	5.0	760	4.68	3.41E-02
ACROS-ELDT-5.0-2	5.0	760	4.69	3.40E-02
ACROS-ELDT-0.01-1	0.010	815	7.72	5.05E-03
ACROS-ELDT-0.01-2	0.010	815	7.71	4.87E-03
ACROS-ELDT-0.1-1	0.10	815	7.64	6.77E-03
ACROS-ELDT-0.1-2	0.10	815	7.64	6.39E-03
ACROS-ELDT-1.0-1	1.0	815	7.36	1.12E-02
ACROS-ELDT-1.0-2	1.0	815	6.63	1.17E-02
ACROS-ELDT-2.0-1	2.1	815	6.21	1.77E-02
ACROS-ELDT-2.0-2	2.1	815	6.30	1.75E-02
ACROS-ELDT-3.0-1	3.2	815	6.42	2.62E-02

ACROS-ELDT-3.0-2	3.2	815	5.75	2.59E-02
ACROS-ELDT-5.0-1	5.0	815	4.67	3.44E-02
ACROS-ELDT-5.0-2	5.0	815	4.68	3.25E-02
ACROS-ELDT-0.01-1	0.010	963	7.79	5.14E-03
ACROS-ELDT-0.01-2	0.010	963	7.86	5.06E-03
ACROS-ELDT-0.1-1	0.10	963	7.71	6.91E-03
ACROS-ELDT-0.1-2	0.10	963	7.72	6.93E-03
ACROS-ELDT-1.0-1	1.0	963	7.46	1.19E-02
ACROS-ELDT-1.0-2	1.0	963	6.58	1.19E-02
ACROS-ELDT-2.0-1	2.1	963	6.33	1.81E-02
ACROS-ELDT-2.0-2	2.1	963	6.41	1.81E-02
ACROS-ELDT-3.0-1	3.2	963	6.60	2.70E-02
ACROS-ELDT-3.0-2	3.2	963	6.02	2.72E-02
ACROS-ELDT-5.0-1	5.0	963	4.62	3.49E-02
ACROS-ELDT-5.0-2	5.0	963	4.63	3.47E-02
ACROS-ELDT-0.01-1	0.010	1067	7.95	5.20E-03
ACROS-ELDT-0.01-2	0.010	1067	7.94	5.14E-03
ACROS-ELDT-0.1-1	0.10	1067	7.81	6.98E-03
ACROS-ELDT-0.1-2	0.10	1067	7.82	6.91E-03
ACROS-ELDT-1.0-1	1.0	1067	7.59	1.19E-02
ACROS-ELDT-1.0-2	1.0	1067	6.65	1.20E-02
ACROS-ELDT-2.0-1	2.1	1067	6.48	1.84E-02
ACROS-ELDT-2.0-2	2.1	1067	6.54	1.82E-02
ACROS-ELDT-3.0-1	3.2	1067	6.69	2.70E-02
ACROS-ELDT-3.0-2	3.2	1067	6.38	2.71E-02
ACROS-ELDT-5.0-1	5.0	1067	4.62	3.49E-02
ACROS-ELDT-5.0-2	5.0	1067	4.65	3.44E-02

389 * Values of pmH reported are calculated by using the correction factors (A_M) from Rai
390 et al. (1995) for pH readings, and conversion factors (Θ) from molarity to molality,
391 $\text{pmH} = \text{pH}_{\text{ob}} + A_M - \log \Theta$ (Xiong et al., 2010). The conversion factors are calculated
392 from densities for NaCl solutions, which are from Söhnel and Novotný (1985).
393
394

395
 396
 397
 398

Table 2. Experimental results concerning solubility of earlandite, $\text{Ca}_3[\text{Citrate}]_2 \cdot 4\text{H}_2\text{O}(\text{s})$, in MgCl_2 solutions produced at SNL at 22.5 ± 0.5 °C.

Experimental Number	Supporting Medium, MgCl_2 , molal	Experimental time, days	pmH*	Solubility expressed as total calcium on molal scale, $m_{\Sigma\text{Ca}}$
ACROS-ELDT-0.01 Mg-1	0.010	203	6.91	7.85E-03
ACROS-ELDT-0.01 Mg-2	0.010	203	6.99	7.87E-03
ACROS-ELDT-0.1 Mg-1	0.10	203	5.70	2.53E-02
ACROS-ELDT-0.1 Mg-2	0.10	203	5.70	2.32E-02
ACROS-ELDT-1.0 Mg-1	1.0	203	4.78	5.30E-02
ACROS-ELDT-1.0 Mg-2	1.0	203	4.79	5.11E-02
ACROS-ELDT-1.5 Mg-1	1.5	203	4.81	5.36E-02
ACROS-ELDT-1.5 Mg-2	1.5	203	4.84	5.34E-02
ACROS-ELDT-2.0 Mg-1	2.0	203	4.99	5.13E-02
ACROS-ELDT-2.0 Mg-2	2.0	203	5.33	5.24E-02
ACROS-ELDT-2.5 Mg-1	2.5	203	5.10	4.98E-02
ACROS-ELDT-2.5 Mg-2	2.5	203	4.86	4.93E-02
ACROS-ELDT-0.01 Mg-1	0.010	385	7.22	7.82E-03
ACROS-ELDT-0.01 Mg-2	0.010	385	7.38	7.69E-03
ACROS-ELDT-0.1 Mg-1	0.10	385	5.34	2.70E-02
ACROS-ELDT-0.1 Mg-2	0.10	385	5.36	2.66E-02
ACROS-ELDT-1.0 Mg-1	1.0	385	4.57	4.66E-02
ACROS-ELDT-1.0 Mg-2	1.0	385	4.69	4.64E-02
ACROS-ELDT-1.5 Mg-1	1.5	385	4.57	4.33E-02
ACROS-ELDT-1.5 Mg-2	1.5	385	4.56	4.56E-02
ACROS-ELDT-2.0 Mg-1	2.0	385	4.71	4.44E-02
ACROS-ELDT-2.0 Mg-2	2.0	385	5.10	4.57E-02
ACROS-ELDT-2.5 Mg-1	2.5	385	4.86	4.22E-02
ACROS-ELDT-2.5 Mg-2	2.5	385	4.41	4.26E-02
ACROS-ELDT-0.01 Mg-1	0.010	458	7.44	7.89E-03
ACROS-ELDT-0.01 Mg-2	0.010	458	7.62	7.87E-03
ACROS-ELDT-0.1 Mg-1	0.10	458	5.58	2.78E-02
ACROS-ELDT-0.1 Mg-2	0.10	458	5.62	2.87E-02
ACROS-ELDT-1.0 Mg-1	1.0	458	4.76	4.59E-02
ACROS-ELDT-1.0 Mg-2	1.0	458	4.81	4.56E-02
ACROS-ELDT-1.5 Mg-1	1.5	458	4.41	4.56E-02
ACROS-ELDT-1.5 Mg-2	1.5	458	4.63	4.59E-02

ACROS-ELDT-2.0 Mg-1	2.0	458	4.90	4.55E-02
ACROS-ELDT-2.0 Mg-2	2.0	458	5.05	4.59E-02
ACROS-ELDT-2.5 Mg-1	2.5	458	4.97	4.28E-02
ACROS-ELDT-2.5 Mg-2	2.5	458	4.60	4.27E-02
ACROS-ELDT-0.01 Mg-1	0.010	660	7.61	7.90E-03
ACROS-ELDT-0.01 Mg-2	0.010	660	7.67	7.58E-03
ACROS-ELDT-0.1 Mg-1	0.10	660	5.56	3.01E-02
ACROS-ELDT-0.1 Mg-2	0.10	660	5.56	3.07E-02
ACROS-ELDT-1.0 Mg-1	1.0	660	4.77	4.88E-02
ACROS-ELDT-1.0 Mg-2	1.0	660	4.81	4.87E-02
ACROS-ELDT-1.5 Mg-1	1.5	660	4.81	4.91E-02
ACROS-ELDT-1.5 Mg-2	1.5	660	4.82	4.89E-02
ACROS-ELDT-2.0 Mg-1	2.0	660	5.01	4.87E-02
ACROS-ELDT-2.0 Mg-2	2.0	660	5.39	4.87E-02
ACROS-ELDT-2.5 Mg-1	2.5	660	5.05	4.65E-02
ACROS-ELDT-2.5 Mg-2	2.5	660	4.71	4.62E-02
ACROS-ELDT-0.01 Mg-1	0.010	709	7.78	8.15E-03
ACROS-ELDT-0.01 Mg-2	0.010	709	7.78	8.04E-03
ACROS-ELDT-0.1 Mg-1	0.10	709	5.60	3.19E-02
ACROS-ELDT-0.1 Mg-2	0.10	709	5.61	3.14E-02
ACROS-ELDT-1.0 Mg-1	1.0	709	4.78	4.96E-02
ACROS-ELDT-1.0 Mg-2	1.0	709	4.80	4.91E-02
ACROS-ELDT-1.5 Mg-1	1.5	709	4.79	4.94E-02
ACROS-ELDT-1.5 Mg-2	1.5	709	4.79	4.79E-02
ACROS-ELDT-2.0 Mg-1	2.0	709	4.99	4.82E-02
ACROS-ELDT-2.0 Mg-2	2.0	709	5.07	4.98E-02
ACROS-ELDT-2.5 Mg-1	2.5	709	5.16	4.79E-02
ACROS-ELDT-2.5 Mg-2	2.5	709	4.72	4.85E-02
ACROS-ELDT-0.01 Mg-1	0.010	758	7.75	8.12E-03
ACROS-ELDT-0.01 Mg-2	0.010	758	7.78	7.78E-03
ACROS-ELDT-0.1 Mg-1	0.10	758	5.58	3.07E-02
ACROS-ELDT-0.1 Mg-2	0.10	758	5.57	3.16E-02
ACROS-ELDT-1.0 Mg-1	1.0	758	4.80	4.93E-02
ACROS-ELDT-1.0 Mg-2	1.0	758	4.94	4.75E-02
ACROS-ELDT-1.5 Mg-1	1.5	758	4.87	5.06E-02
ACROS-ELDT-1.5 Mg-2	1.5	758	4.76	4.99E-02
ACROS-ELDT-2.0 Mg-1	2.0	758	4.92	4.93E-02

ACROS-ELDT-2.0 Mg-2	2.0	758	5.25	5.06E-02
ACROS-ELDT-2.5 Mg-1	2.5	758	5.14	4.85E-02
ACROS-ELDT-2.5 Mg-2	2.5	758	4.63	4.75E-02
ACROS-ELDT-0.01 Mg-1	0.010	813	7.94	8.07E-03
ACROS-ELDT-0.01 Mg-2	0.010	813	7.76	7.85E-03
ACROS-ELDT-0.1 Mg-1	0.10	813	5.72	3.03E-02
ACROS-ELDT-0.1 Mg-2	0.10	813	5.73	3.19E-02
ACROS-ELDT-1.0 Mg-1	1.0	813	4.84	4.94E-02
ACROS-ELDT-1.0 Mg-2	1.0	813	4.88	4.91E-02
ACROS-ELDT-1.5 Mg-1	1.5	813	4.87	4.99E-02
ACROS-ELDT-1.5 Mg-2	1.5	813	4.86	4.99E-02
ACROS-ELDT-2.0 Mg-1	2.0	813	5.06	4.96E-02
ACROS-ELDT-2.0 Mg-2	2.0	813	5.43	4.98E-02
ACROS-ELDT-2.5 Mg-1	2.5	813	5.22	4.77E-02
ACROS-ELDT-2.5 Mg-2	2.5	813	4.79	4.73E-02
ACROS-ELDT-0.01 Mg-1	0.010	961	7.97	8.32E-03
ACROS-ELDT-0.01 Mg-2	0.010	961	7.97	8.06E-03
ACROS-ELDT-0.1 Mg-1	0.10	961	5.88	3.28E-02
ACROS-ELDT-0.1 Mg-2	0.10	961	5.89	3.31E-02
ACROS-ELDT-1.0 Mg-1	1.0	961	4.84	4.97E-02
ACROS-ELDT-1.0 Mg-2	1.0	961	4.88	4.96E-02
ACROS-ELDT-1.5 Mg-1	1.5	961	4.85	3.68E-02
ACROS-ELDT-1.5 Mg-2	1.5	961	4.86	5.02E-02
ACROS-ELDT-2.0 Mg-1	2.0	961	5.05	4.98E-02
ACROS-ELDT-2.0 Mg-2	2.0	961	5.43	4.97E-02
ACROS-ELDT-2.5 Mg-1	2.5	961	5.20	4.79E-02
ACROS-ELDT-2.5 Mg-2	2.5	961	4.77	4.76E-02

399 * Values of pmH reported are calculated by using the correction factors (A_M) from
400 Hansen (2001) for pH readings, and conversion factors (Θ) from molarity to molality,
401 $\text{pmH} = \text{pH}_{\text{ob}} + A_M - \log \Theta$ (Xiong et al., 2010). The conversion factors are from the EQ3
402 output files with the respective MgCl_2 concentrations.
403

404
405
406
407

Table 3. Equilibrium constants at infinite dilution, 25°C and 1 bar, Pitzer interaction parameters in the $\text{Na}^+ - \text{Mg}^{2+} - \text{Ca}^{2+} - \text{Cl}^- - [\text{C}_3\text{H}_5\text{O}(\text{COO})_3]^{3-}$ (or Citrate³⁻) system

Pitzer Parameters					
Species, <i>i</i>	Species, <i>j</i>	$\beta^{(0)}$	$\beta^{(1)}$	C^ϕ	References
Na^+	$\text{Ca}[\text{C}_3\text{H}_5\text{O}(\text{COO})_3]^-$	-0.1310	0.29 ^A	-0.006818	This work
Mg^{2+}	$\text{Mg}[\text{C}_3\text{H}_5\text{O}(\text{COO})_3]^-$	1.0915	1.74 ^A	0	This work
Mg^{2+}	$\text{Ca}[\text{C}_3\text{H}_5\text{O}(\text{COO})_3]^-$	0.3760	1.74 ^A	0	This work
Mg^{2+}	$[\text{C}_3\text{H}_5\text{O}(\text{COO})_3]^{3-}$	0.9330	4.4 ^B	0	This work
Pitzer Mixing Interaction Parameters					
Species <i>i</i>	Species <i>j</i>	Species <i>k</i>	θ_{ij}	ψ_{ijk}	References
Na^+	Ca^{2+}	ClO_4^-	0.07	0.1574	θ_{ij} from data0.fm1; ψ_{ijk} from this work
Equilibrium Constants for Dissolution Reaction of Earlandite and Formation Reaction for $\text{Ca}[\text{C}_3\text{H}_5\text{O}(\text{COO})_3]^-$					
Reaction			$\log K_{sp}$ and $\log \beta_l$ at 25 °C	References	
$\text{Ca}_3[\text{C}_3\text{H}_5\text{O}(\text{COO})_3]_2 \cdot 4\text{H}_2\text{O}$ (earlandite) = $3\text{Ca}^{2+} + 2[\text{C}_3\text{H}_5\text{O}(\text{COO})_3]^{3-} + 4\text{H}_2\text{O}$			-18.1061	This work	
$\text{Ca}^{2+} + [\text{C}_3\text{H}_5\text{O}(\text{COO})_3]^- = \text{Ca}[\text{C}_3\text{H}_5\text{O}(\text{COO})_3]^-$			4.9730	This work	

408
409
410
411
412

^A Values are set according to AP-154, Revision 2 (Xiong, 2013b).

^B The value for $\beta^{(1)}$ is set to 4.4 based on the analog to that for the $\text{Mg}^{2+} - \text{NpO}_2(\text{CO}_3)_2^{3-}$ interaction from FM1.DAT0, which originated from Al Mahamid et al. (1998).

413

414 Figure Captions

415

416 Figure 1. A plot showing experimental total calcium concentrations in equilibrium with
417 earlandite, $\text{Ca}_3[\text{Citrate}]_2 \cdot 4\text{H}_2\text{O}(\text{s})$, in NaCl solutions as a function of experimental time
418 produced in this study.

419

420

421 Figure 2. A plot showing experimental total calcium concentrations in equilibrium with
422 earlandite, $\text{Ca}_3[\text{Citrate}]_2 \cdot 4\text{H}_2\text{O}(\text{s})$, in MgCl_2 solutions as a function of experimental time
423 produced in this study.

424

425

426 Figure 3. A plot showing experimental total calcium concentrations in equilibrium with
427 earlandite, $\text{Ca}_3[\text{Citrate}]_2 \cdot 4\text{H}_2\text{O}(\text{s})$, produced in this study as a function of molalities of
428 NaCl, in comparison with the predicted values based on the model developed in this
429 work.

430

431

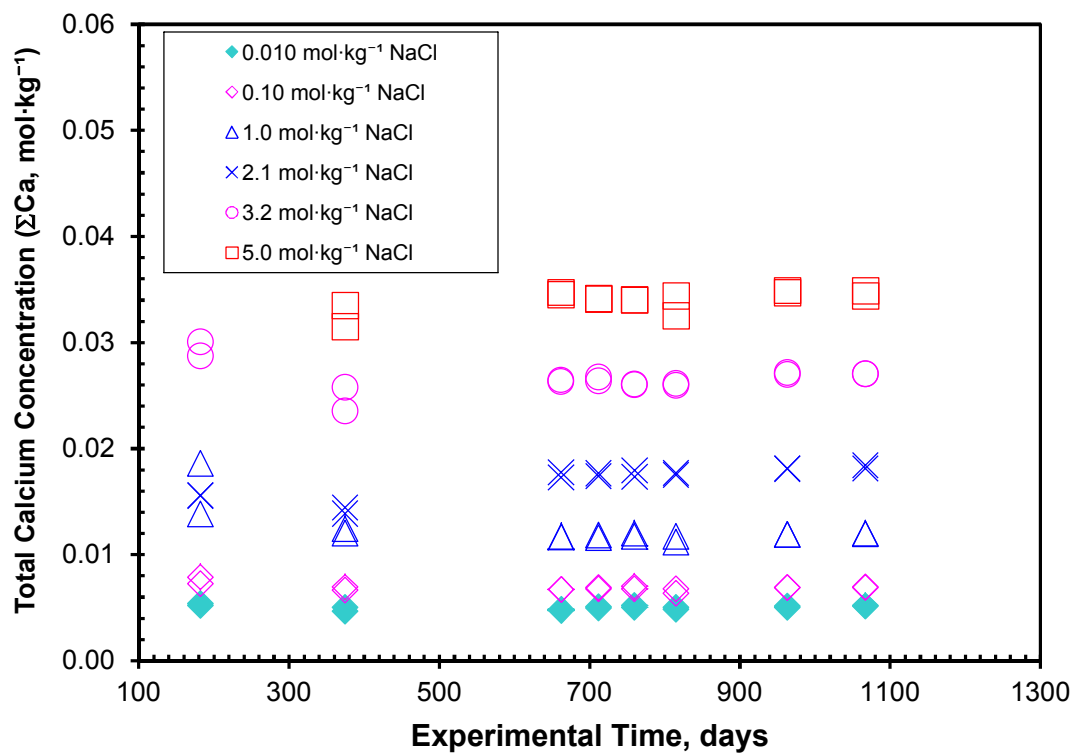
432 Figure 4. A plot showing experimental total calcium concentrations in equilibrium with
433 earlandite, $\text{Ca}_3[\text{Citrate}]_2 \cdot 4\text{H}_2\text{O}(\text{s})$, produced in this study as a function of ionic strengths
434 in MgCl_2 solutions, in comparison with the predicted values based on the model
435 developed in this work.

436

437

438

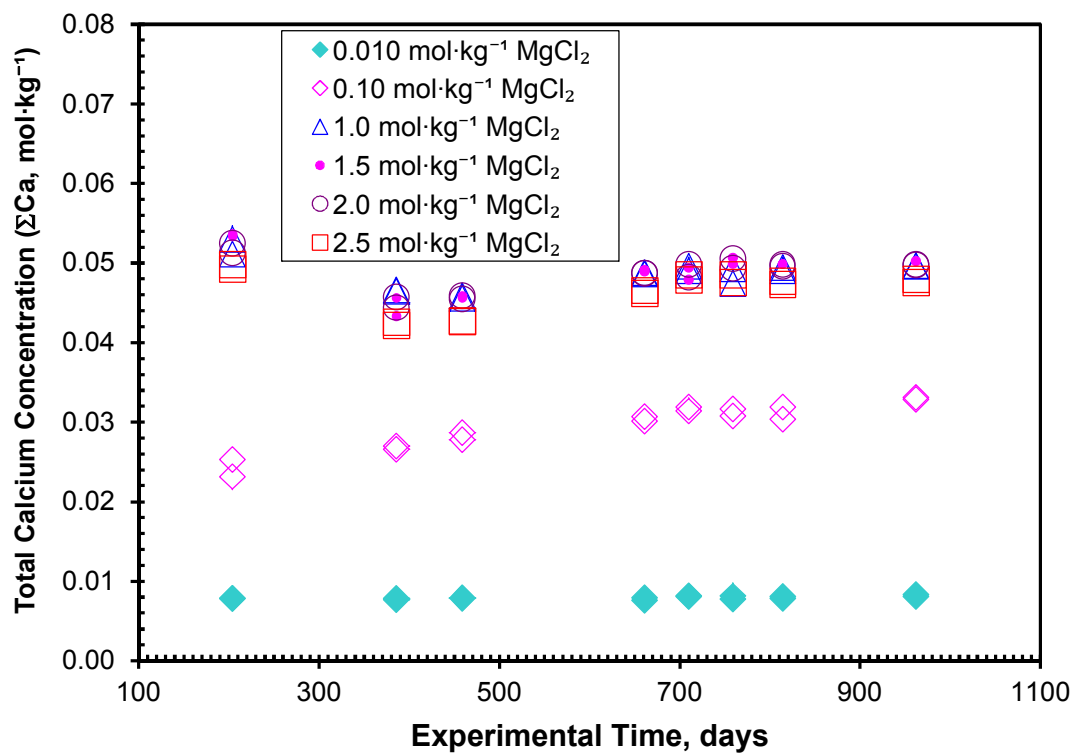
439



440
441
442
443
444

Figure 1.

445



446

447

448 Figure 2.

449

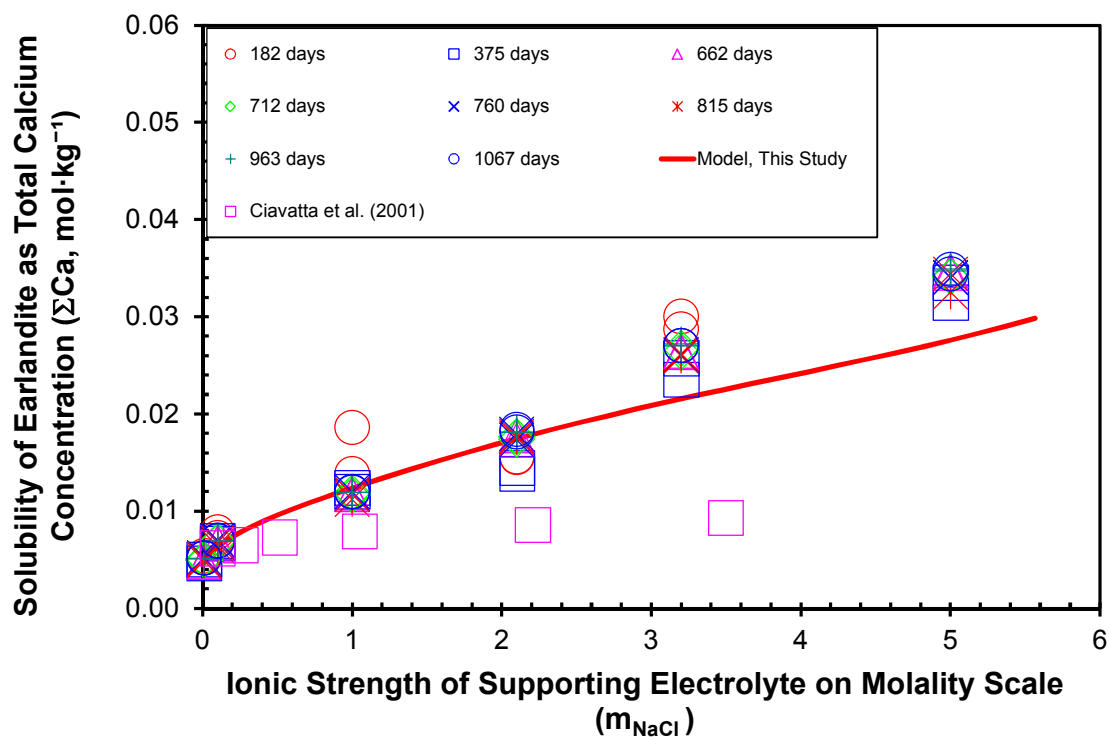
450

451

452

453

454



455

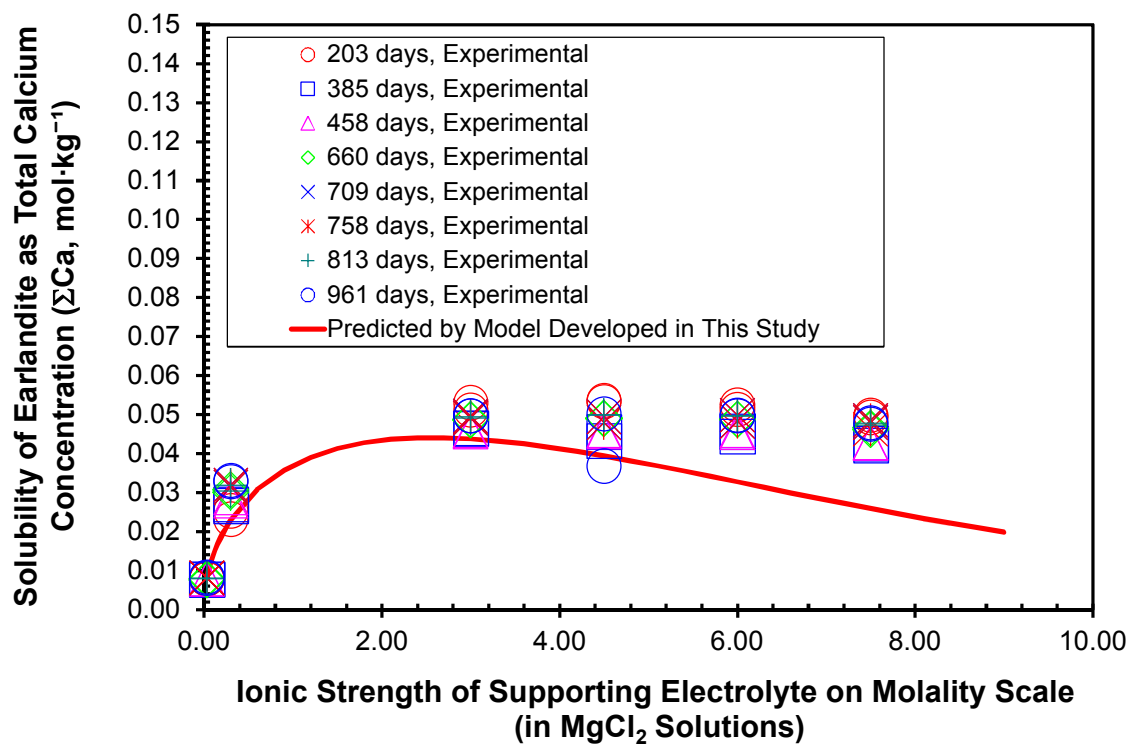
456

457

458

459

Figure 3.



461
462
463
464
465
466

Figure 4.